University of Glasgow

DEPARTMENT OF

AEROSPACE ENGINEERING

Blade Vortex Interaction Studies

by

R.A.McD. Galbraith, F.N. Coton, R.B. Green, C.A. Masson

Blade Vortex Interaction Studies

by

R.A.McD. Galbraith, F.N. Coton, R.B. Green, C.A. Masson

Final contractor report for EPSRC grant number GR/K13547

February 1998

University of Glasgow, Department of Aerospace Engineering, Report 9803

Blade Vortex Interaction Studies

R.A.McD. Galbraith, F.N. Coton, R.B. Green, C.A. Masson
Department of Aerospace Engineering
University of Glasgow
GLASGOW
G12 8QQ

Final contractor report for EPSRC grant number GR/K13547

ABSTRACT

This report contains a summary of the research conducted during the project entitled "Blade Vortex Interaction Studies", EPSRC grant number GR/K13547 in the Department of Aerospace Engineering, University of Glasgow. The original motivation for the study was to provide data to aid understanding of unsteady flows due to blade vortex interaction (BVI), which is a major source of acoustic and aerodynamic problems in helicopter rotor design. In particular knowledge of the effect of blade pitch upon a single vortex interacting with a blade was required. To reflect modern vane tip designs, the effect of a twin vortex system interacting with a blade was also to be studied. To perform the above investigations, a new BVI facility consisting of a rectangular blade instrumented with 72 surface mounted pressure transducers and a vortex generator were constructed which allowed tests at various fixed blade incidences. To provide a simulation of the vane tip vortex system a twin vortex generator was designed and constructed. The resulting data set is unique in its scope and quality, and provides a solid base for further research in this area. A preliminary analysis of the data was presented at an American Helicopter Society specialists' meeting (Masson et al. (1997)), and a journal paper is currently under review (Masson et al (1998)). The data are currently being subjected to a thorough analysis and a number of publications are in preparation.

1. OBJECTIVES

The primary objectives were the construction of a new BVI facility to examine the effects of blade pitch and a twin vortex system upon BVI, to build a high quality data base from the tests, and to perform a basic analysis of the data.

2. METHODOLOGY

The Department of Aerospace Engineering, University of Glasgow, has an established track record in experimental studies of blade vortex interaction. The current research adopted the developed testing approaches directly, and even extended them to reduce wind tunnel time and to deal with the higher number of pressure transducers used in the study. Some smoke flow visualization work was performed, although this was of limited value owing to problems with the performance of the vortex generator at low Reynolds number. Data presentation and analysis was performed on a dedicated, UNIX based platform. To assist with this a graphical user interface was developed.

3. VARIATIONS FROM ORIGINAL PROPOSAL

The main variations from the original proposal were in terms of the timing of the testing and analysis phases. This was essentially due to problems with staff recruitment, wind tunnel scheduling in relation to other ongoing work and breakdowns (most notably a structural failure of a wind tunnel component which led to the destruction of the wind tunnel fan). During most of this downtime much of the analysis software was developed, so that an effective analysis was possible as soon as the data became available. In practice the twin BVI tests were performed immediately after the single vortex tests and the analysis of all the data only occurred towards the end of the contract period. However, a researcher is currently funded by the DERA to perform a more in depth analysis of the data. On the other hand the blade was much more heavily instrumented and the test programme was more comprehensive than originally proposed.

4. DESCRIPTION OF WORK PROGRAMME

4.1 Basic details of rig and rig development during contract period

A schematic diagram of the blade-vortex interaction facility in the University of Glasgow 'Handley Page' wind tunnel is provided in figure 1. The wind tunnel is of the closed return type with a 1.61 x 2.13 octagonal working section. The rig for the experiment basically consisted of a vortex generator, and the rotating blade assembly itself. Two designs of vortex generator were used in the present research, namely the single and twin vortex generators. The blade assembly consisted of a support shaft, which passed through the roof and floor of the wind tunnel. The shaft was rotated by a 1.1kW D.C. motor at 600 rpm. A hub was mounted at the centre span of the shaft which supported the blade, which therefore rotated in the horizontal plane. The hub was counter balanced to reduce dynamic loading on the shaft bearings. Surface mounted pressure transducers were mounted towards the tip of the blade, and these were interfaced to the non-rotating environment using slip rings.

Items retained from the earlier BVI facility at Glasgow were the shafts holding the blade hub and the system providing the blade rotation. The vortex generator (both single and twin), blade and hub were all of a new design. The new single vortex generator

was of the same basic split wing design used in previous experiments at Glasgow; a wing of NACA 0015 section and 0.1524m chord spanned the floor and roof of the tunnel, and the upper portion of the wing was set at an equal and opposite incidence to the lower portion. A single vortex, whose axis is nominally parallel to the tunnel axis, then developed from the junction of the two wing portions. Unlike the previous design, however, the new vortex generator was designed so that the vertical position of the vortex could be set from outside the wind tunnel. This avoided the need to shut down the wind tunnel each time a new vortex height position was required, and resulted in a great time saving during testing. To achieve this the extreme ends of the vortex generator assembly passed through nylatron bearings mounted on the roof and floor of the tunnel. Additional stiffening was provided by pneumatic clamps, which tightened the bearings against the vortex generator. To adjust the height of the vortex above the blade, the pneumatic clamps were released and a digital AC servo motor then moved the vortex generator up and down via a lead screw assembly. This system was controlled by a PC fitted with a National Instruments LAB PC+ data acquisition card programmed using LabVIEW. The motor and PC system were provided by the Department's equipment inventory.

The twin vortex assembly consisted of two cantilever wings, of NACA 0015 cross section and 0.1524m chord, mounted on the floor and roof of the tunnel. Lateral and vertical separation of the vortex cores was achieved by manual adjustment of the position of the wings.

The hub consisted of a single centre piece, which was attached to the shafts. The assembly holding the blade itself was bolted onto the centre piece. This assembly consisted of two halves, which were machined such that when they were placed together they fitted firmly around the blade root. A collar gripped the blade root, and the blade pitch could therefore be altered by loosening bolts that tightened the collar onto the hub assembly. A counterweight was bolted onto the hub centre piece diametrically opposite to the blade.

The blade, of NACA 0015 cross section, chord length 0.1524m and 0.944m span (based on rotor disk radius) was of a carbon fibre/ foam resin construction. Moulds machined from nylatron were used for laying up the blade skins. The blade profile merged to a tapered circular section at the root, such that when attached to the hub, the taper provided the necessary reaction to centrifugal pull-out loading. The surface mounted pressure transducer instrumentation was placed inside a removable tip pod which was then bolted onto the remainder of the blade. This pod contained 72 miniature Kulite pressure tranducers, type CJQH-187, arranged as shown in figure 2. They were arranged to provide a good spatial resolution of both chordwise and spanwise phenomena. The main transducer arrays were at the 78.5% and 98.5% spanwise locations and contained 18 and 12 transducers on the upper and lower surfaces respectively. The subsidiary arrays at 82.5%, 86.5%, 90.5% and 94.5% span contained three transducers each on the upper surface, at the leading and trailing edges and at the mid chord. Short lengths of tubing were used to connect the transducers to the blade surface where necessary, although all the tube lengths were minimized. The transducers were of the differential type; the reference end of the transducer was simply left open inside the tip pod, which was sealed before attachment to the blade. (Note: the transducer offset removal sequence is described later.) The transducer wires from the tip pod passed along the centre of the blade, through the hub and down the shaft to a can positioned at the end of the shaft below the wind tunnel. This can contained anti-alias filters and amplifiers. The signals were then passed to the non-rotating environment via a 36-channel slip ring set; to accomodate the larger number of pressure transducers than slip ring channels a high speed multiplexer was also placed inside the can.

4.2 Instrumentation and data logging system

The data logging system used was identical to that described previously by Galbraith et al. (1995). For the present tests the sampling rate was set at 50kHz per channel; the time skew errors associated with the multiplexing are negligible owing to the anti-alias filters. All data were recorded over a 144° azimuth angle, with 32000 samples logged per channel over 16 revolutions. The synchronization trigger for data acquisition was provided by an optical encoder attached to the rotor shaft. Wind tunnel dynamic pressure was measured using the difference between the working section static pressure and settling chamber pressure. The pressure tappings were connected to a FURNESS FC012 micromanometer which provided an analogue output signal suitable for the data acquisition unit.

The method of removal of offsets from the transducers is particularly important. Each transducer offset contains not only an unloaded contribution but an effect due to centrifugal loading on the transducer medium. The unloaded contribution was taken care of by the method described by Galbraith et al. (1995), with the blade stationary and the wind tunnel shut down. The centrifugal contribution was found by covering the pressure tapping holes with thin tape and then recording the voltages with the blade rotating at 600rpm at each required blade incidence, again with the wind tunnel shut down. This centrifugal offset was then removed as part of the post-processing procedure.

4.3 Test series and procedure

All tests were performed at a nominal maximum blade tip Reynolds and Mach numbers of 600000 and 0.17. The test series is described below.

4.3.1 Single vortex tests

The basic test series for the single vortex is outlined in table 1. z_v is the displacement of the vortex axis from the shaft centre, and y_v is the height of the vortex above the mid chord of the blade. Five rotor pitch angles were considered. For each pitch angle a parallel interaction ($z_v/c=0$) and two oblique interactions were studied ($z_v/c=\pm 2$). For the zero pitch case the vortex heights were set at 33 positions (in steps of 0.1c in the range $-1.0 < y_v/c < -0.2$ and $0.2 < y_v/c < 1.0$ and in steps of 0.025c in the range $-0.2 < y_v/c < 0.2$). At the other pitch settings the vortex height was set at 13 positions as follows:

$$y_v/c = \pm 1.0, \pm 0.8, \pm 0.6, \pm 0.4, \pm 0.2, \pm 0.1, 0.0$$

Vortex strengths are indicated in table 1.

In addition to the tests above, tests with the blade set at the various pitch angles were performed with the vortex generator removed from the wind tunnel.

4.3.2 Twin vortex tests

Prior to these tests the behaviour of the twin vortex system in the wind tunnel was investigated. With the blade and shaft assembly removed from the wind tunnel, the velocity field at various positions downstream of the vortex generators was measured using a cross wire probe mounted on a 2-D traverse. Data were collected using a TSI IFA 300 hot wire system connected to a Pentium PC. Detailed results of this survey are described by Copland et al. (1997) Using the results of this study the vortex generators could be positioned to give the correct vortex locations in the interaction plane.

The test series is outlined in table 2. For the twin vortex tests the blade was set at 0° pitch only. The vortex generators were positioned so that the generator tips described a circle of diameter d. The angle that the line between the two tips made with the horizontal is the angle δ. The centre of the generator circle was set at the $z_v/c=0.0$ position and at heights $y_v/c=0.0$ and ± 0.2. For each case the turning circle diameter was set at 0.5c, 0.75c and 1.0c. The nominal angular positions are given in table 2. The vortex strength of each generator was set at 2.9 m^2s^{-1}, so that the overall strength of the twin vortex system may be compared with that of the single vortex tests.

4.3.3 Data storage, reduction and presentation

All the binary data were stored on the acquisition PC before being loaded onto a DAT tape. The raw data on the DAT tape were then reduced on a SUN SPARC 10 workstation using a dedicated code written in C. Centrifugal offsets were removed, and the data were non-dimensionalised with respect to the rotor tip velocity. The reduced data were identified by a run number. From previous tests it was realised that there were significant differences in the data collected for consecutive revolutions during the same run. This was the result of vortex meander about the nominal vortex position (Horner et al. (1994)). Therefore the data from the sixteen revolutions per run were only averaged when absolutely necessary.

Significant effort was put into the development of the presentation and analysis software, basically to assist with internal archiving and to increase accessibility to the data in the future. FORTRAN code was used to calculate the integrated force and moment coefficients, while the presentation and analysis software was written using PV WAVE. This software allowed the construction of a graphical user interface permitting easy access to the various display/analysis options.

5. SAMPLE RESULTS AND PRELIMINARY ANALYSIS

The salient features from a preliminary analysis of the single and twin vortex test series are described below

5.1 Single vortex tests

Figure 3 shows typical pressure data recorded at the inboard station (r/R=0.785) during a parallel interaction ($z_v/c=0$). The chordwise pressure distribution is shown as a function of non-dimensional time, x_v/c. (x_v is the distance of the leading edge of the blade at the spanwise position being considered to the vortex axis).For clarity only every 5th pressure sample is shown. In each plot the vortex height was set at $y_v/c = 0.1$, which results in the vortex trajectory passing above the rotor disk. The vortex strength was set at the maximum value of $\Gamma=5.8$ m^2s^{-1}.

Figure 3a shows the blade at 0° pitch. As the vortex approaches the blade the leading edge suction initially rises slowly; the pressure rise is due to the flow field induced by the vortex. As the vortex moves onto and over the forward portion of the blade the suction collapses rapidly. After approximately $x_v/c = 0.35$ a more clearly defined suction ridge is observed, which is associated with vortex convection over the blade surface. The ridge ends as the vortex leaves the blade at approximately $x_v/c=0.92$. After the vortex passes ocer the trailing edge a disturbance may be seen in the trailing edge region of the blade. This may be due to the effects of the vortex passing over the trailing edge (Coton et al. (1997)), or it may be due to resonance in the pressure transducer/ tube system. The latter possibility is unlikely owing to the filtering applied to the transducer signals.

Similar features to above are observed for the 6° and 12° pitch cases shown in figures 3b and 3c. In fact the only significant difference is in the mean suction level, which can be attributed to the bound circulation associated with the fixed, non-zero blade pitch.

Figure 4 shows the sectional normal force coefficient behaviour for the above pressure data. As expected C_n increases as the vortex approaches the blade. It reaches a maximum at about $x_v/c = 0$, and then decreases rapidly before reaching a plateau. This is caused by the direct suction effect of the vortex offsetting the reduction in aerodynamic incidence of the blade as the vortex moves towards the trailing edge. The point at which the vortex moves off the trailing edge is indicated by the dashed line (this was taken from the pressure plots of figure 3.) The sharp drop in C_n just prior to $x_v/c=1.0$ therefore occurs after the vortex has passed over the trailing edge. This drop is due to the loss of the suction effect described above. An obvious feature of the effect of blade pitch is in the overall magnitude of the normal force coefficient; this is due to bound circulation effects.

An important parameter in blade vortex interaction studies is the ΔC_n magnitude, i.e. the difference between the maximum and minimum C_n due to BVI. The effect of blade pitch upon this parameter was determined from the data. However the vortex induced effect upon C_n needed to be isolated from the blade pitch effect upon C_n. This was achieved by subtracting the C_n behaviour of a vortex free test from the BVI test at the same blade pitch. Figure 5 shows the effect of vortex height upon ΔC_n as a function of blade pitch with the vortex effect isolated from the bound circulation. At large vortex heights the vortex induced effect is small, and the maximum ΔC_n is observed at $y_v/c = 0.1$. This offset is mainly due to the sudden drop in C_n as the vortex passes over the trailing edge, as described above. Figure 5 indicates that, to a first order at least, vortex induced effects are independent of blade pitch angle for a given vortex height and strength. This observation is reinforced by the remarkable qualitative similarity in pressure data and load data features.

The quarter chord pitching moment behaviour during BVI is shown in figure 6 for a blade pitch of 12°. As the vortex approaches the blade, C_m increases and reaches a peak at about $x_v/c = 0.1$; this delay is thought to be due to a greater net suction on the forward portion of the blade as the vortex first convects onto the rotor. As the vortex convects over the blade C_m falls and becomes negative (nose down), and the vortex induced suction peak moves towards the trailing edge. After the vortex passes over the trailing edge there is a large increase in C_m; this is due to a combination of the loss in suction causing the sudden drop in C_n described above and the long moment arm. The peak value of C_m itself increases as the blade pitch increases, although this increase is not a vortex induced effect.

5.2 Twin vortex tests

Figure 7 shows BVI pressure data for the twin vortex system for a nominal vortex separation of one chord length with $\delta = 15^o$ and $\Gamma_{total} = 5.8m^2s^{-1}$. The presence of the twin vortex system is shown clearly by the twin suction peaks and vortex convection ridges, which implies that the two vortices passed over the upper surface of the blade. This result is consistent with the 15° inclination of the vortex pair. The separation of the twin peaks indicates a vortex separation of 1.1 chord lengths, indicating that the vortex separation has increased during the interaction. This effect is thought to be due to the effect of the rotor on the twin vortex system, since Copland et al. (1997) found that vortex separation remained approximately constant for 10 chord lengths downstream of the vortex generators in an otherwise empty wind tunnel.

The initial growth in suction on figure 7 may be thought of as due to a far field effect, in which the combined rotational flow field of the twin vortex system is the same as that due to a single vortex of the same strength. This is reflected by the leading edge C_p value of -1 at the beginning of the sampling sequence, which is similar to the value for the single vortex test on figure 2a. As the twin vortex system approaches the blade, however, the flow field becomes dominated by the first vortex of the pair, and this causes the observed increased growth in suction. Thereafter the BVI is dominatd by the local effect of the vortex over the blade surface. The second interaction has a similar appearance to the first, but the reduced suction levels indicate that the vortex is higher above the blade surface than the first.

An interesting result shown on figure 7 is the magnitude of the first suction peak. In spite of the individual vortex strengths being half that of the single vortex case shown in figure 3a, the peak C_p magnitudes of the single and twin vortex cases are almost the same at $|C_p| \approx 2.5$. This effect is thought to be due to vortex meander, in which the position of the vortices change with time; for the remaining revolutions of the run shown in figure 7 the suction peaks were different, and in most cases lower, which would be expected for vortex meander.

Normal force data from the test shown in figure 7 are shown in figure 8. The dashedlines represent where the two vortices pass over the trailing edge of the blade. The overall appearance of the C_n behaviour due to the first interaction is similar to the single vortex test. However, the collapse in C_n as the vortex passes behind the leading edge is less than that of a single vortex case, essentially because of the increase in blade aerodynamic incidence caused by the approach of the second vortex. As the first vortex passes over the trailing edge, however, the dip in C_n can still be seen. This loss of lift is quickly recovered as the second vortex approaches the leading edge, and there is a second collapse in C_n as this vortex passes behind the leading edge. The C_n level after this collapse is lower than that associated with the first vortex, basically because of the lack of upwash (indeed the first vortex will now induce a downwash). There is no observable dip in C_n after the second vortex passes over the trailing edge, which reflects the greater height of this vortex above the blade surface than the first. An interesting observation is

that in spite of the peak suction lavels being comparable to the single vortex test of the same combined strength, the ΔC_n values are much lower for the twin vortex test.

Quarter chord pitching moment data from the test shown in figure 7 are shown in figure 9. The initial behaviour as the first vortex approaches the blade is similar to the single vortex case. However, as the second vortex approaches C_m stays positive. A sudden nose-up moment is induced as the first vortex passes over the trailing edge, and C_m increases again as the second vortex becomes closer to the blade. There is a slight increase in C_m as this vortex passes over the trailing edge. Comparison of the twin BVI C_m data withthe single vortex case shows, in general, reduced magnitudes in the variations of C_m.

6. CONCLUSIONS

A new blade vortex interaction facility has been developed which has allowed a thorough parametric study of the effects of blade pitch and a twin vortex system upon blade vortex interaction phenomena. The blade was instrumented to a high spatial resolution so that spanwise and chordwise phenomena could be investigated. A preliminary analysis has revealed that for single vortex BVI the vortex induced effects are to a first order independent of blade pitch for a given vortex height. For a twin vortex system reduced normal force and pitching moment coefficients were observed compared to the single vortex case. Some results have been published or are under review for publication, and further analysis of the data is proceeding under a DERA grant.

7. REFERENCES

Copland, C.M., Coton, F.N. & Galbraith, R.A.McD. (1997) "An Experimental Study on the Idealised Vortex System of Novel Rotor Blade Tip" 20th European Rotorcraft Forum, Berlin, september 1997.

Coton, F.N., Galbraith, R.A.McD., Grant, I. & Hurst, D. (1997) "Analysis of Complex Flow Fields by Animation of PIV and High Resolution Unsteady Pressure Data" RTO/ AGARD Fluid Dynamics Panel Symposium, Advanced Aerodynamic Measurement Technology, September 1997

Galbraith, R.A.McD., Coton, F.N., Jiang, D. & Gilmour, R. (1995) "Preliminary Results from a Three-Dimensional Dynamic Stall Experiment of a Finite Wing" 21st European Rotorcraft Forum, St. Petersburg, Russia, Sept. 1995

Horner, M.B., Stewart, J.N., Galbraith, R.A.McD., Grant, I. & Coton , F.N. (1994) "An Examination of Vortex Deformation During Blade-Vortex Interaction Utilising Particle Image Velocimetry" 19th Congress of the International Council of the Aeronautical Sciences, Anaheim, CA, Sept. 1994

Masson, C.M., Green, R.B, Galbraith, R.A.McD. & Coton, F.N. (1997) "An Experimental Study of a Loaded Blade Interacting with Single and Twin Vortices" Proceedings of the American Helicopter Society Technical Specialists' Meeting for Rotorcraft Acoustics and Aerodynamics, Ft. Magruder Inn, Williamsburg, VA, Oct. 1997

Masson, C.M., Green, R.B, Galbraith, R.A.McD. & Coton, F.N. (1998) "An Experimental Study of a Loaded Blade Interacting with a Single Vortex" submitted to the Aeronautical Journal

Rotor pitch/ deg	z_v/c	Vortex strength/ m^2s^{-1}
0	-2	5.8
	0	5.8
	2	5.8
3,6,9,12	-2	±5.8, ±3.7
	0	±5.8, ±4.6, ±3.2, ±2.6
	2	±5.8, ±5.2

Table 1 Basic test matrix for single vortex tests

Vortex strength m^2s^{-1}	Height of vortex pair centroid	d/c	δ/ deg
5.8	-0.2	0.5	0,15,30,45,60,70,90 105,120,135,145,150
		0.75	0,45,90,135
		1.0	0,45,90
	0.0	0.5	0,15,30,45,60,70,90 105,120,135,145,150
		0.75	0,15,30,45,60,70,90,135
		1.0	0,15,30,45,60,70,90,105,120
	0.2	0.5	0,15,30,45,60,70,90 105,120,135,145,150
		0.75	0,45,90,135
		1.0	0,45,90

Table 2 Test matrix for twin vortex tests

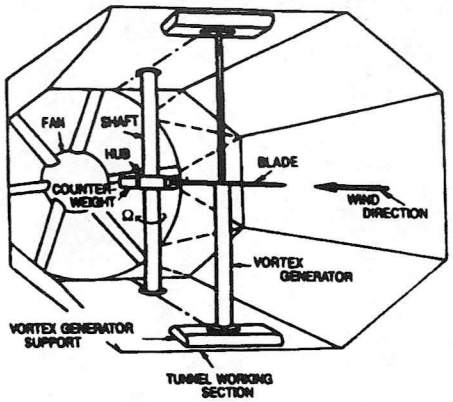

Figure 1 University of Glasgow BVI facility

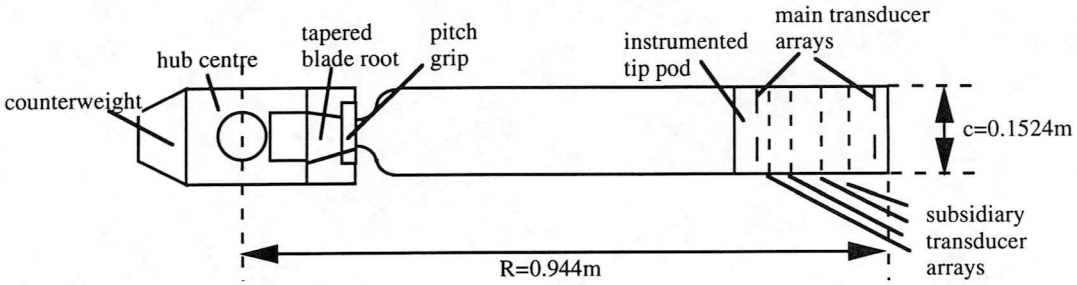

Figure 2 Blade and hub arrangement

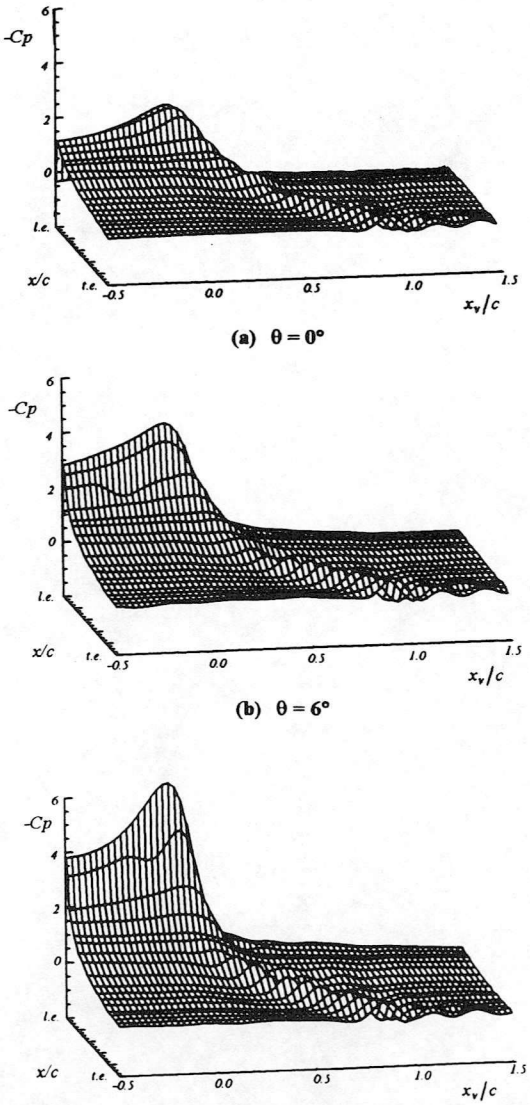

Figure 3 Upper surface chordwise pressure distribution at 78.5% span location as a function of time for single vortex, parallel BVI. $y_V/c = 0.1$, $\Gamma = 5.8 m^2 s^{-1}$. Figures a, b and c are for blade pitch of 0°, 6°, and 12° respectively.

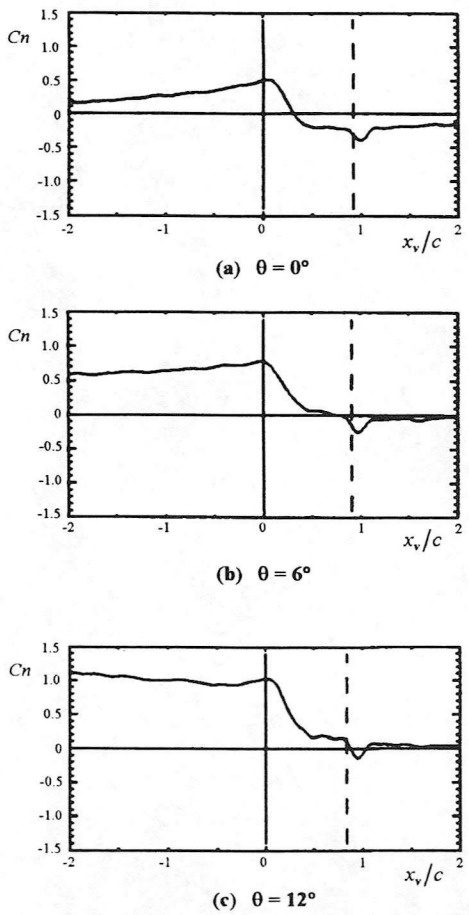

Figure 4 Normal force behaviour at 78.5% span location as a function of time during single vortex, parallel BVI. $y_V/c = 0.1$, $\Gamma = 5.8 m^2 s^{-1}$. Figures a, b and c are for blade pitch of 0°, 6°, and 12° respectively.

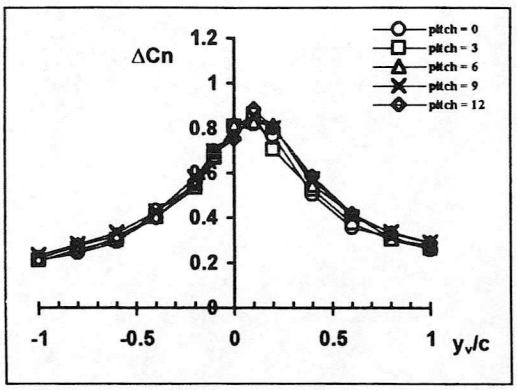

Figure 5 Vortex induced ΔC_n for single vortex, parallel BVI as a function of vortex height for $\Gamma = 5.8 m^2 s^{-1}$. The effect of blade pitch is shown.

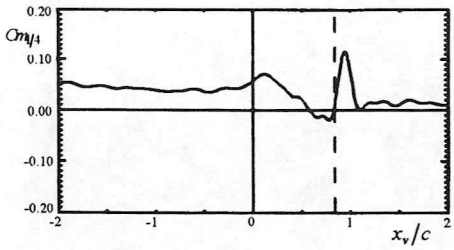

Figure 6 Quarter chord pitching moment behaviour at 78.5% span location as a function of time during single vortex, parallel BVI. $y_V/c = 0.1$, $\Gamma = 5.8 m^2 s^{-1}$, blade pitch = 12°.

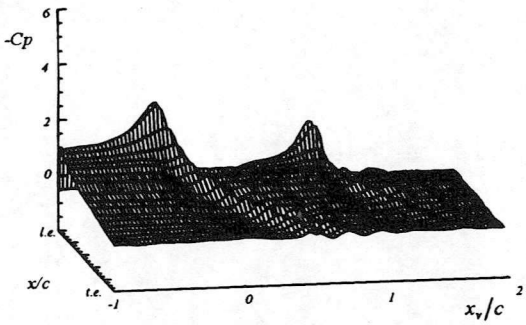

Figure 7 Upper surface chordwise pressure distribution at 78.5% span location as a function of time for twin BVI. $y_V/c = 0.1$, $d/c = 0.1$, $\Gamma = 2.9 m^2 s^{-1}$, $\delta = 15^o$. The blade is at zero degrees pitch.

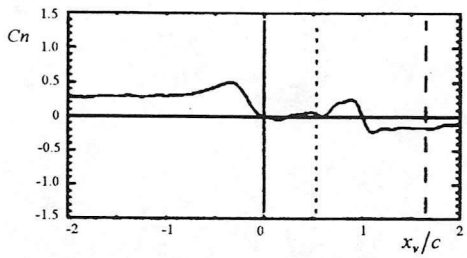

Figure 8 Normal force behaviour at 78.5% span location as a function of time for twin BVI. $y_V/c = 0.1$, $d/c = 0.1$, $\Gamma = 2.9 m^2 s^{-1}$, $\delta = 15^o$. The blade is at zero degrees pitch.

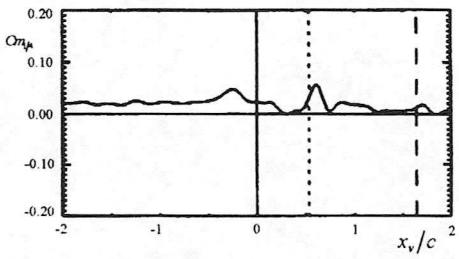

Figure 9 Quarter chord pitching moment behaviour at 78.5% span location as a function of time for twin BVI. $y_V/c = 0.1$, $d/c = 0.1$, $\Gamma = 2.9 m^2 s^{-1}$, $\delta = 15^o$. The blade is at zero degrees pitch.